Formal Methods for
Reasoning and Uncertainty Reduction in Evidential Grid Maps

Andreas Grimmer[a], Joachim Clemens[b], Robert Wille[a]

[a]*Institute for Integrated Circuits, Johannes Kepler University, Linz, Austria*
[b]*Cognitive Neuroinformatics, University of Bremen, Bremen, Germany*

Abstract

Information fusion is the task of combining data collected from different sources into a unified representation. Here, a main challenge is to deal with the inherent uncertainty contained in the information, such as sensor noise, conflicting information, or incomplete knowledge. In current approaches, one usually employs independence assumptions in order to reduce the complexity. Because of this, the full potential of the gathered data is often not fully exploited and the fusion may lead to additional uncertainty. In order to reduce this uncertainty, further information in form of background and expert knowledge can be utilized, which is often available for real-world scenarios. However, reasoning on this knowledge is a computational complex task. In this work, we propose a methodology which utilizes formal methods for that reasoning, which allows to relax some of the independence assumptions. We demonstrate the proposed methodology using evidential grid maps – a belief function-based environment representation, in which different kinds of uncertainty are represented explicitly. Our methodology is evaluated based on basic structures as well as on real-world data sets. The results show that the uncertainty in the maps is significantly reduced by considering dependencies among cells.

Keywords: Uncertainty Reduction, Formal Methods, Information Fusion, Belief Functions, Occupancy Grid Maps

1. Introduction

When a technical system acts in or interacts with an environment, it relies on a suitable representation of this environment. In many practical applications, the required information is provided by multiple sources, such as sensory data or expert knowledge. Additionally, information fusion techniques [1] are usually needed to create a unified representation. One of the largest research fields on this topic is mobile robotics [2], where the robot collects data using its sensors and builds a spatial representation of its environment.

In the past decades, many different representation forms have been proposed and even more approaches were developed to build these from scratch [3]. The algorithms have to evaluate the data from different sources with respect to their uncertainty (e.g. sensor noise, conflicting

information, and incomplete or missing knowledge) and, afterwards, derive the most accurate representation from it, which is compatible with all provided information. Obviously, this is a complex task, since practically relevant environment sizes reaches from tens to thousands of meters and typical sensors provide a huge amount of data every second. Both lead to a large combinatorial complexity. In order to make the computation feasible, most approaches use restrictive independence assumptions, such as conditional independencies of particular parts in the environment. As a consequence, these algorithms cannot exploit the full potential of the data (later, Section 3 illustrates and discusses this in more detail).

In this work[1], we propose the exploitation of formal methods to address this issue. Formal methods are well-known for their capabilities to efficiently traverse and prune large search spaces. In particular, we exploit the deductive power of *maximum satisfiability solvers* (MAX-SAT, [5, 6]) in order to consider dependencies among different parts of the environment, which are dropped by standard approaches for the reasons discussed above. This allows us to use expert knowledge about the environment to reduce the uncertainty in the derived results and to infer the true state of the corresponding parts of the environment.

We apply the proposed methodology to occupancy grid maps [7], a popular spatial representation in robotics. In particular, we are using evidential grid maps [8], which are based on the belief function theory [9] and are well suited for navigation tasks [10, 11]. Furthermore, they explicitly represent different kinds of uncertainty [12], which provide additional information to our methodology that is not present in probabilistic grid maps. We demonstrate how the proposed methodology reduces the uncertainty by using expert knowledge about the environment. In particular, we apply our approach in the context of evidential grid maps representing office environments. More precisely, a set of hand-crafted benchmarks containing basic room structures as well as two real-world maps are used as benchmarks in our evaluations.

The reminder of this paper is structured as follows: In Section 2, we review the background on evidential grid maps and information fusion using this kind of maps. In Section 3, the limitations of the current approaches are discussed and a motivation for the proposed methodology is provided. In Section 4, we present our general idea, while in Section 5, we describe the solution in detail. In Section 6, the results of an empirical evaluation using small structures as well as real-world datasets are presented and discussed. The paper concludes with a summary and an outlook.

2. Background

This section reviews the background on occupancy grid maps in general and evidential grid maps in particular. Afterwards, the corresponding fusion process is re-visited, which is applied in order to generate a more precise grid map from the combination of data. Finally, we present how we convert evidential grid maps into a categorical representation for using them as input for the methodology proposed in this work. In order to ease the descriptions, we keep the considered models as simple as possible.

2.1. Evidential Grid Maps

One particular and frequently used spatial environment representation are *occupancy grid maps* [7], which distinguishes between empty and occupied areas in the environment.

---

[1]This work extends a previous conference paper [4].

Definition 1. *An* occupancy grid map *represents a spatial environment in terms of a discretized grid, where each grid cell may either be empty (denoted by e) or occupied (denoted by o).*

The information on whether a cell is empty or occupied is obtained from different sources, e.g. gathered by sensors, prior knowledge, etc. Because these sources of information may be afflicted with uncertainty (e.g. sensor noise, contradictory sensor measurements among different sensors or over time, vague expert knowledge, or the simple non-availability of information), a formalism to represent uncertain information in a given map is required. To this end, the state of a cell is usually modeled probabilistically with a single occupancy probability distribution $P(o)$. Here, for example, $P(o) = 0.3$ represents that the corresponding cell in the grid may be occupied with probability of 30%, what implies that it may be empty with probability of 70% ($P(e) = 0.7$), since the probability theory requires that $P(o) + P(e) = 1$.

The proposed methodology, however, benefits from an explicit representation of different dimensions of uncertainty, since e.g. the complete lack of information cannot explicitly be expressed by probabilities. A uniform distribution ($P(e) = 0.5$ and $P(o) = 0.5$) could work, but bears the risk of being misinterpreted with the fact that the cell is considered to be empty/occupied with probability of 50% due to conflicting measurements. Therefore, the belief function theory [9, 13], which is often considered as a generalization of the well-known Bayesian probability theory, is used in this work. This theory allows us to assign belief mass not only to the singletons of a hypotheses space (here e and o), but also to all subsets including $\{e, o\}$ and $\emptyset$. The belief mass is assigned using so-called *mass functions*, which are defined as follows.

Definition 2. *Let Θ be the frame of discernment, i.e. the hypotheses space, and $A \subseteq \Theta$ a hypothesis of Θ. Then, a* mass function *is a mapping $m : \mathcal{P}(\Theta) \to [0, 1]$ assigning a mass value to each hypothesis A of Θ such that*[2]

$$\sum_{A \subseteq \Theta} m(A) = 1. \tag{1}$$

In terms of an evidential grid map, the frame of discernment is defined as

$$\Theta = \{e, o\} \tag{2}$$

and a mass function indicating the state of a grid cell is defined as

$$m(A) \in [0, 1], \quad \forall A \subseteq \Theta, \tag{3}$$

while satisfying Eq. (1).

The belief function theory allows for explicitly stating different dimensions of uncertainty [12]. More precisely,

- certain information can be represented by assigning mass to e or o,

- a lack of information can be expressed by assigning mass to the disjunction $\{e, o\}$ (i.e. Θ), and

- conflicting information can be expressed by assigning mass to the empty set (i.e. $\emptyset$).

---

[2]Note that we are using unnormalized mass functions here, which allow $m(\emptyset) \neq 0$.

In contrast, the probability theory can express uncertainty only by the ratio between $P(e)$ and $P(o)$. For example, a complete lack of information and conflicting information are both mapped to a uniform distribution and are therefore indistinguishable as discussed above.

Example 1. *Figure 1a shows an example of an evidential grid map m_1 as it could have been derived from sensory data. The four quadrats within a cell indicates the masses on e, o, Θ, and $\emptyset$. As shown, the bottom left part is well observed with high mass assigned empty (e) and occupied (o). However, a significant amount of uncertainty exists in the remainder of this map, where high mass is assigned Θ, indicating a lack of information.*

2.2. Information Fusion

In order to reduce the amount of uncertainty in the map and to build a complete representation of the environment, information is usually gathered from more than one source. The information sources can be from different types or from the same type and collected over time. This results in several maps, which, eventually, have to be *fused* into a unified representation. This process is called *information fusion* or, in the context of multiple sensors, *multi-sensor fusion*. A consistent consideration of the uncertainty of the different maps is thereby required.

There are several works on information fusion to build evidential grid maps using different types of sensors, including sonar [8, 14, 15], laser scanners [16, 17], and radar [18]. Besides of robotics, evidential grid maps have also been created from sensory data in automotive applications [19, 20, 21, 22, 23]. However, the algorithms focus on the mapping problem only and assume that the pose, i.e. the position and orientation of the robot gathering the data, is known. Accordingly, they do not consider the full joint estimation problem of building an environment map and simultaneously consider the respective *localization*. However, for example in robotics, both issues frequently have to be solved at the same time. In other words, *Simultaneous Localization And Mapping* (SLAM, [24]) is required.

In [25], an approach to model the SLAM problem in the belief function theory has been proposed as a generalization of the successful FastSLAM algorithm [26, 27]. The approach was further improved and applied to path planning and active exploration in [11]. In general, the algorithm allows one to use different combination rules [9, 13, 28, 29, 30]. A comparison of different rules in the context of evidential mapping can be found in [15, 17] and in the context of evidential SLAM in [25]. However, the *conjunctive rule of combination* [13] is the only one that yields mass on $\emptyset$ and, hence, allows for a representation of conflicting evidence.[3] Because of that, this rule is applied in the following consideration.

Definition 3. *Let m_1 and m_2 be two mass functions defined over the same frame of discernment Θ and induced by two distinct pieces of evidence. The combination (fusion) of these two mass functions with the conjunctive rule of combination $\bigcirc$ results in the mass function $m_{1\bigcirc2} = m_1 \bigcirc m_2$ which is defined as*

$$m_{1\bigcirc2}(A) = \sum_{B\cap C=A} m_1(B)m_2(C), \quad \forall A \subseteq \Theta. \tag{4}$$

---

[3]There exist different interpretations on the meaning of the mass on $\emptyset$. Our interpretation is closely related to the particular application and a detailed discussion on this topic can be found in [11, 12].

For mass functions in the context of evidential grid maps that are defined over $\Theta = \{e, o\}$, the conjunctive rule of combination reduces to

$$m_{1 \odot 2}(A) = \begin{cases} m_1(A)m_2(A) + m_1(A)m_2(\Theta) + m_1(\Theta)m_2(A), & \text{if } A = \{o\}, \{e\}, \\ m_1(\Theta)m_2(\Theta), & \text{if } A = \Theta, \\ 1 - \sum_{B \in \mathcal{P}(\Theta) \setminus \emptyset} m_{1 \odot 2}(B), & \text{if } A = \emptyset. \end{cases} \tag{5}$$

Example 2. *In order to reduce the uncertainty of the map m_1 from Figure 1a, further data has been gathered, resulting in a second map m_2 as shown in Figure 1b. Applying the conjunctive rule of combination in Eq. (5) results in the fused representation $m_{1 \odot 2}$ shown in Figure 1c.*

Here, all cells with high mass on e or o in both *input maps have high mass on the respective set in the fused map as well (see e.g. cell $(0, 4)$ or cell $(3, 1)$). But, beyond that, uncertainty is reduced in all cells with high mass on Θ in only* one *of the input maps (see e.g. cell $(0, 2)$ or cell $(4, 3)$). In contrast, new conflicts arise when the input maps contain contradictory evidences. This is the case e.g. for cell $(4, 0)$ where $m_1(\{e\}) = 0.9$ and $m_2(\{o\}) = 0.9$, which is fused to $m_{1 \odot 2}(\emptyset) = 0.8$ – representing another dimension of uncertainty.*

2.3. Evidential Grid Maps with Categorical Mass Functions

The use of MAX-SAT solvers, as proposed in the next sections, requires the input to be Boolean or pseudo-Boolean. For this reason, we are using categorical mass functions as input for our methodology. Those are defined as follows.

Definition 4. *Let Θ be the frame of discernment, i.e. the hypotheses space, and $A \subseteq \Theta$ a hypothesis of Θ. Then, a* categorical mass function *is a mapping $m : \mathcal{P}(\Theta) \to \{0, 1\}$ assigning a mass value to each hypothesis A of Θ such that*

$$\sum_{A \subseteq \Theta} m(A) = 1. \tag{6}$$

A categorical mass function in the context of evidential grid maps indicates the state of a grid cell as

$$m(A) = \begin{cases} 1, & \text{if } A = B, \\ 0, & \forall A \subseteq \Theta \setminus B, \end{cases} \quad B \subseteq \Theta. \tag{7}$$

In order to convert an evidential grid map consisting of non-categorical mass functions to an evidential grid map that contains only categorical ones, the mass of each cell is assigned the set with the highest value, i.e.

$$m(A) = \begin{cases} 1, & \text{if } A = B, \\ 0, & \forall A \subseteq \Theta \setminus B, \end{cases} \quad B = \arg\max_{C \subseteq \Theta} m'(C), \tag{8}$$

where m' denotes the non-categorical mass function of a single cell and m is the resulting categorical mass function.

Example 3. *To use the fused map $m_{1 \odot 2}$ from Figure 1c as input for our methodology, the mass functions of its cells are converted to categorical ones using Eq. (8). The resulting map is shown in Figure 1d, where the symbols in the cells indicate that the mass value of the respective set is $1 -$ implying that the mass on all other $A \subseteq \Theta$ is 0. For example, $m_{1 \odot 2}(\{e\}) = 0.9$ in cell $(0, 4)$ results in all mass assigned e, $m_{1 \odot 2}(\{o\}) = 0.9$ in cell $(3, 1)$ results in all mass assigned o, $m_{1 \odot 2}(\Theta) = 0.8$ and $m_{1 \odot 2}(\Theta) = 0.7$ in cell $(0, 2)$ and cell $(4, 3)$, respectively, results in all mass assigned Θ, and, finally, $m_{1 \odot 2}(\emptyset) = 0.8$ in cell $(4, 0)$ results in all mass assigned $\emptyset$.*

Legend of a non-categorical cell

$m(e)$	$m(o)$
$m(\Theta)$	$m(\emptyset)$

(a) Initial map m_1

(b) Further map m_2

(c) Fused map $m_{1\circledcirc 2}$

(d) Categorical map of $m_{1\circledcirc 2}$

Figure 1: Obtained information in terms of evidential grid maps.

3. Motivation

Information fusion as reviewed in the previous section is an effective method to combine different sources of information and to reduce the uncertainty of grid maps. However, the full potential of the gathered data is not exploited by simply fusing the information to a combined representation, since some areas may remain unexplored. Moreover, it may lead to additional uncertainty when the combined mass functions conflict each other. In order to resolve these conflicts and to further reduce the uncertainty of the maps, additional information in the form of background and expert knowledge can be applied, which is often available for real-world scenarios.

For example, in an office building, robots usually find a certain amount of empty space to move on (i.e. sub-grids of cells with mass on e) that, in turn, is divided by walls (i.e. sub-grids of cells with mass on o). This background and expert knowledge can be utilized to conclude that

- an uncertain cell which is surrounded by empty cells likely is empty as well or

- an uncertain cell within a "line" of occupied cells likely belongs to a wall and, hence, is occupied as well.

Typical structures like those can be utilized in terms of *further rules*. By this, much more precise maps with less uncertainty may result.

Example 4. *Consider again the representation of the fused information $m_{1 \odot 2}$ shown in Figure 1d. Applying the information provided by the rules sketched above allows us to conclude that*

- *the unknown cell $(1, 3)$ with mass on Θ is empty, because most of the neighboring cells (in fact, all of them) are empty as well (i.e. have their mass on e),*

- *the unknown cell $(2, 1)$ with mass on Θ is occupied, because it is in a line with occupied cells (i.e. cells with mass on o), and*

- *the conflict in cell $(4, 0)$ with mass on $\emptyset$ may be resolved in favor of map m_2, since this cell is in a line with occupied cells (i.e. cells with mass on o) and, hence, is very likely occupied as well.*

Various of such rules can be derived. However, their application may lead to contradictions, e.g. when a rule implies that a cell has to be empty while another rule implies that it has to be occupied. In fact, this might be the case for cell $(2, 1)$ in Figure 1d. As discussed in Example 4, this cell is assumed to be occupied due to the "wall"-rule described above. But besides that, also the "empty subgrid"-rule (assuming this cell to be empty) might be applicable, since most of the neighboring cells are empty. Because of this, different priorities are assumed for each rule. In this work, we formalize this as follows.

Definition 5. *Let R be the set of* all *rules, which can be applied to all cells in a given grid map. For each rule $r \in R$, an additional* weight w_r *is provided which represents the priority of rule r against other rules $r' \in R \setminus \{r\}$.*

Based on these priorities, a subset $\hat{R} \in \mathcal{P}(R)$ of rule combinations is desired which does not introduce new conflicts and maximizes the overall weight. More formally,

- for a given mass assignment m of a map, $\hat{R}$ shall not lead to new mass on $\emptyset$ and

- all remaining subsets $R' \in \mathcal{P}(R) \setminus \hat{R}$ that also do not introduce new conflicts have to have a smaller or equal overall weight, i.e. $w_{R'} \leq w_{\hat{R}}$ with $w_R = \sum_{r \in R} w_r$.

Following this optimization criteria, as much as possible further information is concluded while, at the same time, new conflicts are avoided.

However, determining $\hat{R}$ obviously is a computationally complex task: For each combination of rules, all possible mass assignments to all grid cells have to be considered. Since a total of $|\mathcal{P}(R)| = 2^{|R|}$ combinations are possible, this results in an exponential complexity.

Furthermore, the combination of different sources is a complex task on its own, even without considering additional rules. Each cell has a combinatorial complexity of $|\mathcal{P}(\Theta)| = 2^{|\Theta|}$, which results in $|\mathcal{P}(\Theta)|^M = 2^{|\Theta| M}$ possible maps, where M is the number of cells. In order to handle this complexity, all solutions proposed thus far apply significant restrictions, including pure grid mapping with known pose and probabilistic grid maps [7], the original FastSLAM algorithm [26], its variants for building probabilistic grid maps [27, 31], and the Evidential FastSLAM algorithm with belief function grid maps as considered here [11]. In particular, all these approaches apply a so-called (conditional)[4] independence assumption, which factorizes the joint distribution over all grid cells into marginal cell distributions. More precisely,

$$m^Y(A) = \prod_{i=1}^{M} m^{Y_i}(A), \quad \forall A \subseteq \Theta \tag{9}$$

is applied, where m^Y is the mass function for the complete map Y and m^{Y_i} is the mass function for a single cell Y_i. This allows one to update the cells independently of each other which reduces the complexity from the high-dimensional space of all maps $|\mathcal{P}(\Theta)|^M$ to single cells $M \cdot |\mathcal{P}(\Theta)|$. On the downside, however, it prevents one to express any dependencies among cells. As a consequence, none of the rules sketched above would be applicable under this assumption.

In this work, we propose a methodology, which relaxes the independence assumption after the initial fusion process and applies additional rules as sketched above to dissolve uncertainties in the fused map. The application of rules, but also a propagation of information would not be possible when each cell is considered independently. The following example demonstrates this.

Example 5. *Consider the input map represented in Figure 2a, which allows to apply the "empty subgrid"-rule only on cell $(1, 1)$ because this cell has 6 or more neighbor cells also being empty. This results in the intermediate result shown in Figure 2b. The obtained information now allows to apply the "empty subgrid"-rule again, namely on cell $(2, 2)$. This can similarly propagate to cells $(2, 1)$ and $(3, 1)$, eventually yielding the map shown in Figure 2d. This example demonstrates how the derived mass assignments can propagate and how these derived assignments can be used for further application of rules.*

Overall, considering all combination of rules is a computationally complex task, but it leads to the best possible result based on the available information and rules.

4. General Idea

As discussed in the previous section, obtaining the best possible utilization of background and expert knowledge (provided in terms of rules) for a fused map is a computationally complex

---

[4]For simplification, the conditional part is omitted here. See [11] for the full equations.

3 | e | e | e | e 　　　　**3** | e | e | e | e 　　　　**3** | e | e | e | e

2 | e | e | Θ | e 　　**2** | e | e | Θ | e 　　**2** | e | e | e | e

1 | e | Θ | Θ | Θ 　**1** | e | e | Θ | Θ 　　. . .　　**1** | e | e | e | e

0 | e | e | e | e 　　　**0** | e | e | e | e 　　　　**0** | e | e | e | e

　　0　1　2　3　　　　　　0　1　2　3　　　　　　　0　1　2　3

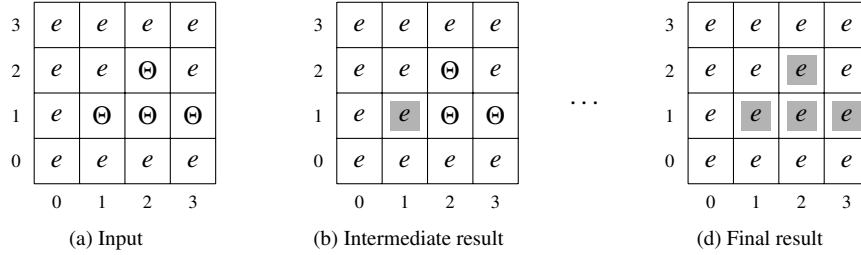　　(a) Input　　　　(b) Intermediate result　　　(d) Final result

Figure 2: Demonstration of rule propagations.

problem. For this purpose, all possible combinations of rules have to be considered. For a set of rules R, this multiplies together to a search space of $2^{|R|}$ different combinations to be explored, i.e. an exponential complexity.

To cope with this complexity, we propose to exploit the deductive power of formal methods. Their intelligent decision heuristics, powerful learning schemes, and fast implication methods allow to efficiently traverse large search spaces. They have been proven to be very effective for many practically relevant design problems such as equivalence checking [32], property checking [33], or automatic test pattern generation [34]. Our thesis is that this deductive power can also be utilized in order to determine the best solution from all the possible rule combinations. To this end, we particularly utilize solvers for the *weighted MAX-SAT* problem [5, 6].

The *weighted MAX-SAT* problem is an extension of the *Boolean satisfiability* (SAT) problem. Both problems are defined as follows:

Definition 6. *The* Boolean satisfiability problem *determines an assignment to the variables of a Boolean function* $\Phi : \{0, 1\}^n \rightarrow \{0, 1\}$ *such that* Φ *evaluates to* 1 *or proves that no such assignment exists. The function* Φ *is thereby given in* Conjunctive Normal Form *(CNF). Each CNF is a conjunction of clauses where each clause is a disjunction of literals and each literal is a propositional variable or its negation. A CNF is satisfied if all clauses are satisfied, a clause is satisfied if at least one literal is satisfied, and a positive (negative) literal is satisfied if the corresponding variable is set to 1 (0).*

Definition 7. *Let* Ψ *be a set of weighted clause pairs* (r_i, w_i) *with* r_i *being an actual clause (i.e. a disjunction of literals) and* w_i *an associated weight. Then, the* weighted MAX-SAT problem *determines an assignment such that the total weight of the satisfied clauses is maximized. These clauses are so-called* soft constraints*. In addition to the soft constraints, it is possible to define a set of clauses that are mandatory to be satisfied as in the pure satisfiability problem, so-called* hard constraints.

Example 6. *Let* $\Phi = (x_1 + x_2 + \overline{x}_3)(\overline{x}_1 + x_3)(\overline{x}_2 + x_3)$. *Then,* $x_1 = 1, x_2 = 1,$ *and* $x_3 = 1$ *is a satisfying assignment solving the SAT problem.*

Accordingly, let $\Psi = \{(\overline{x}_1 + \overline{x}_2, 2), (x_1, 4), (\overline{x}_1 + x_2, 3)\}$. *Then,* $x_1 = 1$ *and* $x_2 = 1$ *is a solution to the MAX-SAT problem, maximizing the total weight to* 7.

Note that the required representation, i.e. the CNF clauses, can easily be derived from any Boolean function in linear time (see e.g. [35] and [36]). Hence, for sake of clarity we provide the following formulations in general pseudo-Boolean algebra.

9

5. Symbolic Representation

Instead of naively enumerating and checking all possible combinations, we are formulating the question what combination of rules leads to the best possible information in terms of a MAX-SAT problem. Therefore, we first formulate a symbolic representation of the fused map that then allows us to formulate the rules as constraints.

5.1. Symbolic Formulation of the Fused Map

The symbolic formulation has to represent all possible states of the fused map, i.e. all possible mass assignments of the respective cells.

Definition 8. *Consider a fused grid map m^Y of size $w \times h$, where w is the width and h is the height of the map. Then, all possible states of this map are symbolically represented by four-valued variables c_{xy} with $0 \le x \le w - 1$ and $0 \le y \le h - 1$, where*

- *$c_{xy} = e$ represents that the cell at (x, y) is assumed to be empty (i.e. $m^{Y_{xy}}(\{e\}) = 1$),*

- *$c_{xy} = o$ represents that the cell at (x, y) is assumed to be occupied (i.e. $m^{Y_{xy}}(\{o\}) = 1$),*

- *$c_{xy} = \Theta$ represents that the state of the cell at (x, y) is unknown (i.e. $m^{Y_{xy}}(\Theta) = 1$), and*

- *$c_{xy} = \emptyset$ represents that the state of the cell at (x, y) is conflicting (i.e. $m^{Y_{xy}}(\emptyset) = 1$).*

Here, Y_{xy} denotes the cell at position (x, y) and $m^{Y_{xy}}$ is the corresponding mass function.

Since this representation eventually has to be passed to a MAX-SAT solver, which accepts Boolean input variables only, we apply a four-valued formulation: Each variable c_{xy} is actually represented by two Boolean variables c_{xy}^1 and c_{xy}^0. All constraints proposed in the following are formulated accordingly.

The resulting set of c_{xy}-variables constitutes an initial MAX-SAT instance, which is entirely composed of unbounded variables and represents all possible states of the considered map. Next, this symbolic representation is restricted based on the available information. In fact, some assignments are already pre-defined by the fusion process. This is incorporated by employing the *hard* constraints

$$c_{xy} = e \tag{10}$$

or

$$c_{xy} = o \tag{11}$$

for each cell (x, y) whose information is already certain (i.e. which has mass $m^{Y_{xy}}(\{e\}) = 1$ or mass $m^{Y_{xy}}(\{o\}) = 1$, respectively). All other variables remain unrestricted for now. This results in a MAX-SAT instance which symbolically represents all possible instances of the map left to be considered.

Example 7. *Consider again the map from Figure 1d. Applying the formulation from above results in a symbolic representation as sketched in Figure 3a. A "?" denotes cells whose information from the fusion process is considered to be uncertain.[5] Certain information on these cells are now supposed to be determined by the MAX-SAT solver based on further rules derived from background and expert knowledge.*

---

[5]Due to the artificial nature of the considered example (aimed for illustrating all issues in a simple fashion), the amount of uncertainty is relatively small.
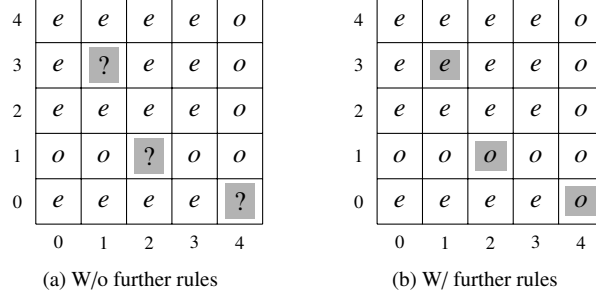
4	e	e	e	e	o
3	e	?	e	e	o
2	e	e	e	e	o
1	o	o	?	o	o
0	e	e	e	e	?
	0	1	2	3	4

(a) W/o further rules

4	e	e	e	e	o
3	e	e	e	e	o
2	e	e	e	e	o
1	o	o	o	o	o
0	e	e	e	e	o
	0	1	2	3	4

(b) W/ further rules

Figure 3: Solutions obtained by the MAX-SAT solver.

5.2. Default Cell Assignments

Passing the MAX-SAT instance formulated above to a corresponding solving engine would lead to an arbitrary assignment to the remaining c_{xy}-variables representing the state of the cells denoted by "?". Since we are not interested in arbitrary assignments, we employ a rule in the formulation that, by default, sets all cells to their respective uncertainty value. More precisely, for each uncertain cell (x, y) the *soft* constraint $(r_{xy}^{default}, w^{default})$ is added to the instance. The added rule depends on the uncertainty value, i.e. it is

$$r_{xy}^{default} := c_{xy} = \Theta \tag{12}$$

for cells with $m^{Y_{xy}}(\Theta) = 1$, and

$$r_{xy}^{default} := c_{xy} = \emptyset \tag{13}$$

for cells with $m^{Y_{xy}}(\emptyset) = 1$. Note that these rules are not explicitly enforced, but realized as *soft* constraints, which can but do not have to be enforced by the MAX-SAT solver during the search process.

5.3. Incorporation of the Rules

Much more important are rules which are based on the background and expert knowledge, e.g. the "empty subgrid"-rule as well as the "wall"-rule discussed in Section 3. The "empty subgrid"-rule is formulated for an uncertain grid cell at position (x, y) as a soft constraint $(r_{xy}^{empty}, w^{empty})$ with

$$r_{xy}^{empty} := \left(\sum_{(x',y') \in NB(x,y)} c_{x'y'} = e \right) \geq 6 \wedge \left(\sum_{(x',y') \in NB(x,y)} m^{Y_{x'y'}}(\{e\}) \right) \geq 3 \wedge c_{xy} = e, \tag{14}$$

where the function $NB(x, y)$ gives the set of all neighbor cells of the position (x, y). In order that this rule evaluates to true and therefore is applied, the following three conditions have to be satisfied: (1) at least six neighbors are assumed to be empty, (2) three neighbors have to be fixed as empty by the fused grid map m^Y (this ensures that the application of the rule is based on initial information provided by the fused map and not only on results of a propagation of rule applications),[6] and (3) the considered cell at position (x, y) has to be empty as well. The required

---

[6]Note that, if cell (x, y) is in a corner or an edge of the grid, the values 6 and 3 are adjusted accordingly.

number of neighbors which are assumed to be empty or have to be fixed as empty can be adjusted depending on the considered maps. Note that applying this "empty subgrid"-rule on the cell at position (x, y) disallows the solver to simultaneously apply one of the "default"-rules on this cell.

Analogously, the "wall"-rule is formulated for an uncertain grid cell at position (x, y) as a soft constraint $(r_{xy}^{wall}, w^{wall})$ with

$$
\begin{aligned}
r_{xy}^{wall} := \Bigg\{ & \left(\sum_{x'=0}^{x-1} c_{x'y} = o + \sum_{x'=x+1}^{w-1} c_{x'y} = o \right) = w - 1 \wedge \left(\sum_{x'=0}^{x-1} m^{Y_{x'y}}(\{o\}) + \sum_{x'=x+1}^{w-1} m^{Y_{x'y}}(\{o\}) \right) \geq w \cdot 0.7 \vee \\
& \left(\sum_{y'=0}^{y-1} c_{xy'} = o + \sum_{y'=y+1}^{h-1} c_{xy'} = o \right) = h - 1 \wedge \left(\sum_{y'=0}^{y-1} m^{Y_{xy'}}(\{o\}) + \sum_{y'=y+1}^{h-1} m^{Y_{xy'}}(\{o\}) \right) \geq h \cdot 0.7 \Bigg\} \\
& \wedge c_{xy} = o.
\end{aligned}
\tag{15}
$$

In order that this rule evaluates to true, either the row or the column in which the considered cell is located, has to be completely assumed occupied and information of e.g. 70% of the cells have to be provided by the initially given fused map (again in order to avoid an unwanted propagation of rule applications). Additionally, the considered cell itself has to be occupied as well. The respective amounts of cells can be adjusted depending on the considered map here as well. Note that this rule depends on the grid size (i.e. the variables h and w), which is always known.

Although the information fusion process is based on multiple initial maps, it is possible that the resulting fused map still contains areas which are completely unexplored, i.e. $m^{Y_{xy}}(\Theta) = 1$ for multiple neighboring positions (x, y). For cells in these areas, usually no information shall be derived by rules. This implemented by the "unexplored"-rule $(r_{xy}^{unexplored}, w^{unexplored})$ with

$$
r_{xy}^{unexplored} := m^{Y_{xy}}(\Theta) \wedge \left(\sum_{(x',y') \in NB(x,y)} m^{Y_{x'y'}}(\Theta) \right) = 8 \wedge c_{xy} = \Theta
\tag{16}
$$

This rule ensures that a cell with its initial mass assigned Θ and whose neighbor cells are assigned Θ as well is not changed. It is assigned a high weight $w^{unexplored}$ compared to the other rules. Note that this rule explicitly distinguishes between uncertainty caused by missing information and uncertainty caused by conflicting information. It is not reasonable to infer something based on vacuous information in a region that was not observed so far. In contrast, a conflict (i.e. mass on $\emptyset$) indicates that the robot has collected information about the corresponding region already. Accordingly, the methodology should try its best do reduce this uncertainty by the use of the other rules. Both cases are indistinguishable when a Bayesian grid map is used and, as a consequence, it would not be possible to formulate the "unexplored"-rule.

All presented rules allow to handle a certain amount of erroneous data, since they do not require that all cells satisfy a specific constraint. For example, the presented "empty subgrid"-rule requires that only 6 of 8 neighbors of a cell are assigned empty in order to derive that this cell is empty as well. In addition, all rules use multiple cells to derive a single cell, which makes the rules robust to erroneous data.

5.4. Determining the Best Combination of the Rules

Rules as introduced above as well as other ones derived from further background and expert knowledge can be applied to each cell (x, y), which defines the total set of rules R, i.e.

$$R = \bigcup_{x=0}^{w-1} \bigcup_{y=0}^{h-1} \{(r_{xy}^{default}, w^{default}), (r_{xy}^{empty}, w^{empty}), (r_{xy}^{wall}, w^{wall}), (r_{xy}^{unexplored}, w^{unexplored})\}. \qquad (17)$$

This set R represents all soft-constraints, which have to be considered by the MAX-SAT solver. But obviously not all of them can be enforced at the same time (as discussed several times above). Therefore, the MAX-SAT solver is used to determine the activation of the rules for which the sum of the weights is maximized and, therefore, represents the best combination of the rules.

Example 8. *Consider again the map from Figure 1d and its symbolic representation sketched in Figure 3a. Furthermore, it is assumed e.g. by an expert that the highest weight is assigned the "unexplored"-rule, the second highest weight is assigned the "wall"-rule, and the third highest weight is assigned the "empty grid"-rule. The "default"-rules have the lowest weight. Employing the proposed formulations leads to an optimal satisfying solution from which the map shown in Figure 3b can be derived. Here, all the uncertainties are removed. More precisely:*

- *Cell $(1, 3)$ is assumed to be empty due to rule r_{13}^{empty}.*

- *For cell $(2, 1)$, two rules can be applied, namely r_{21}^{wall} and r_{21}^{empty}. However, since the weight of the "wall"-rule w^{wall} is higher than the weight of the "empty grid"-rule w^{empty}, this cell is assumed to be occupied.*

- *Finally, the conflict in cell $(4, 0)$ is resolved with rule r_{40}^{wall}, since the weight of the "wall"-rule w^{wall} is higher than the weight of the "default"-rule $w^{default}$.*

Results like this are obtained in a significantly more efficient fashion by MAX-SAT solvers than e.g. by simple enumeration.

6. Experimental Evaluation and Case Study

The proposed methodology has been implemented in Java resulting in a method for reasoning and uncertainty reduction in evidential grid maps. To this end, the solver Z3 [37] has been utilized, which provides a MAX-SAT implementation based on [38]. All experiments have been conducted on a 3.8 GHz Intel Core i7 machine with 32GB of memory running 64-bit Ubuntu 16.04. In the following, we summarize our evaluation setup and the obtained results.

6.1. Evaluation Setup

This section provides the details of the evaluation setup, i.e. the considered benchmarks, the selected rules, the used quality criteria, and the used baseline. Based on this setup, we evaluate whether the proposed methodology is able to correctly reduce the uncertainty in evidential grid maps and we compare the results with a baseline.

Considered Benchmarks. As benchmarks, we consider hand-crafted benchmarks (Section 6.2) containing basic room structures (e.g. maps composed of occupied and vacant spaces like walls and floors) as well as two real-world maps (Section 6.3) generated by the Evidential FastSLAM algorithm [11]. The hand-crafted benchmarks allow us to generate various wall elements and to randomly add uncertainties into the maps. Thus, we can evaluate the proposed methodology with respect to different structures and different degrees of uncertainty. The two real-world maps demonstrate the usefulness of the proposed methodology for realistic and practical relevant scenarios.

Selection of the Rules. The proposed methodology presented above describes four rules, which are suitable for room structures with walls. However, it is not restricted to this kind of map and can be extended with other and more advanced, map-specific rules. In fact, the used rules have to be selected and developed depending on the given maps (i.e. their structures and their allocation of the uncertainty). For example, if the maps also contain chairs and desks, specialized rules may be useful, which ensure that chairs and desks always consist of exactly four legs.

For our evaluations, we generalized the above described "wall"-rule (see Eq. 15) in order to also support (1) diagonal walls and (2) walls, which do not span the entire grid. This enhanced rule allows to represent composite wall structures (e.g. rooms, wall projections, doors). It is also configurable with respect to the wall length (i.e. the number of occupied cells which have to be in a row/column or diagonal so that it is detected as a wall). This parameter depends on the structure of the map and its resolution.

The weights of the rules control how "aggressively" they are applied compared to other rules. Rules with high weights are more likely that they get applied. How to configure the weights depends again on the given map and the used rules. In our evaluations, we experimentally considered different weights of the rules and, eventually, derived a good compromise. Additionally, we exemplarily show how different weights change the results.

Quality Criteria. In order to evaluate the quality of the resulting maps, we use different criteria. For defining these quality criteria, the following three maps are required:

- The *fused map* represents the input for the proposed methodology. The corresponding mass function is denoted as m^Y in the following.

- The *derived map* represents the output after applying the proposed methodology. The corresponding mass function is denoted as m^D in the following.

- The *ground truth map* represents the reality, which is, of course, not known to the methodology. The corresponding mass function is denoted as m^{GT} in the following.

Using these three map types, we can formally define the quality criteria. Therefore, we define a cell at position (x, y) in the fused map to be *uncertain*, if the constraint

$$uncrt_{xy} := \{(m^{Y_{xy}}(\Theta) \vee m^{Y_{xy}}(\emptyset)\} \wedge \{m^{GT_{xy}}(\{o\}) \vee m^{GT_{xy}}(\{e\}))\} \tag{18}$$

is satisfied. This constraint ensures that the value of the considered cell in the input map is unknown (i.e. either Θ or $\emptyset$) and, additionally, ensures that the same cell in the ground truth map is occupied or empty (i.e. it is actually part of the environment).

This allows us to define

Table 1: The used confusion matrix.

$\sum_{x=0}^{w-1}\sum_{y=0}^{h-1}$	$m^{D_{xy}}(\{o\})$	$m^{D_{xy}}(\{e\})$
$m^{GT_{xy}}(\{o\})$	TP	FN
$m^{GT_{xy}}(\{e\})$	FP	TN

- the percentage of *correctly* derived cells, i.e.

$$CorD := \frac{\sum_{x=0}^{w-1}\sum_{y=0}^{h-1} uncrt_{xy} \wedge \{m^{D_{xy}}(\{o\}) \wedge m^{GT_{xy}}(\{o\}) \vee m^{D_{xy}}(\{e\}) \wedge m^{GT_{xy}}(\{e\})\}}{\sum_{x=0}^{w-1}\sum_{y=0}^{h-1} uncrt_{xy}}, \quad (19)$$

- the percentage of *wrongly* derived cells, i.e.

$$WroD := \frac{\sum_{x=0}^{w-1}\sum_{y=0}^{h-1} uncrt_{xy} \wedge \{m^{D_{xy}}(\{o\}) \wedge m^{GT_{xy}}(\{e\}) \vee m^{D_{xy}}(\{e\}) \wedge m^{GT_{xy}}(\{o\})\}}{\sum_{x=0}^{w-1}\sum_{y=0}^{h-1} uncrt_{xy}}, \quad (20)$$

- and the percentage of *not* derived cells, i.e.

$$NotD := 1 - (CorD + WroD). \quad (21)$$

Using these quality criteria, it is possible to define the ratio between correctly and wrongly derived cells (i.e. the *accuracy*) as

$$ACC := \frac{CorD}{CorD + WroD}. \quad (22)$$

The accuracy is the most important quality criterion for evaluating the proposed methodology as it states how accurately the used rules derive information on the mass of cells. For example, an accuracy of 100% denotes that the assignments of all derived cells are equal to the assignments specified in the ground truth map (and, hence, are equal to the reality).

Moreover, we define a confusion matrix to further evaluate the performance. We use this confusion matrix to evaluate if the proposed methodology confuses *occupied* and *empty* cell assignments. The confusion matrix is defined as shown in Table 1, where the actual class is represented by the ground truth map *GT* and the predicted class is represented by the derived map *D*. Furthermore, "positive" is associated with occupied and "negative" with empty.

For example, true-positive (TP) specifies the percentage of *uncertain* cells, which are derived as occupied and are occupied in the reality as well (specified by the ground truth map). False-negative (FN) specifies the percentage of *uncertain* cells, which are derived as empty but are occupied in reality. True-negative (TN) and false-positive (FP) are defined analogously.

Based on the values of the confusion matrix, we additionally provide

- the *true positive rate* (i.e. $TPR := \frac{TP}{TP+FN}$) and

- the *true negative rate* (i.e. $TNR := \frac{TN}{FP+TN}$).

Baseline. We implemented a filter in order to compare the obtained results with a baseline. This filter tries to reduce uncertainties by summing up the occurrences of the different categorical mass functions in the neighborhood of an uncertain cell. Then, the maximal occurred value is assigned as the new value to the considered cell. It therefore uses all eight adjacent neighbor cells to reduce the uncertainty of a cell.
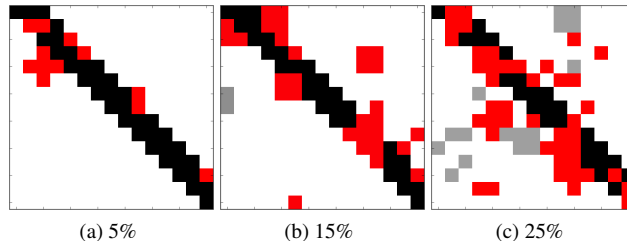
| (a) 5% | (b) 15% | (c) 25% |

Figure 4: Input maps with different levels of uncertainties.

6.2. Basic Structures

First, we evaluated the quality of the derived maps using hand-crafted benchmarks of basic room structures such as doors, corners, and diagonal walls which have a size of 15×15. These hand-crafted maps initially do not contain uncertainty (i.e. all cells are either occupied or empty). Therefore, we randomly insert uncertain cells and uncertain areas (consisting of multiple adjacent cells) by replacing fixed assigned cells. This allows us to evaluate the proposed methodology with different amounts of uncertain cells. In order to simulate real measurements, grid cells next to walls are more likely to have mass assigned $\emptyset$ than other grid cells because, in these areas, real measurements are more likely to conflict each other due to sensor noise. Therefore, the percentage of grid cells with mass on $\emptyset$ is higher than the percentage of grid cells with mass on Θ. Furthermore, in order to minimize the statistical error of the randomly modified maps, we conducted all experiments ten times and report the average values.

For each benchmark, we provide three different settings of uncertainties. In particular, the amount of unknown and conflicting cells either is approx. 5%, 15%, or 25% of the total number of cells. To illustrate the different levels of uncertainties, Figure 4 shows three sample input maps. In these maps (and also all following maps), black cells denote mass on o, white cells denote mass on e, red cells denote mass on $\emptyset$, and gray cells denote mass on Θ.
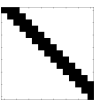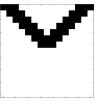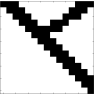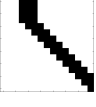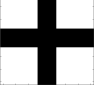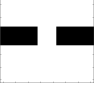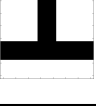
Table 2 shows the obtained results. In all configurations, the accuracy for the proposed methodology as well as for the baseline is higher than 85%, which means that most of the derived cells match the value of the ground truth map. Overall, we can summarize that the proposed methodology and the baseline produce results of similar quality for the basic room structures.

6.3. Application to Real-World Maps

Finally, we evaluated the proposed methodology on two real-world maps. These two maps are generated by Evidential FastSLAM [11] from data collected by wheel-driven robots, which were equipped with laser scanners (180° field of view, 1° angular resolution) and were navigated through indoor environments. Since the mass functions in the evidential maps estimated by Evidential FastSLAM are not categorical, we convert them to categorical ones using Eq. (8) before we use the maps as input for the proposed methodology.

As mentioned in Section 6.1, a generalized *wall*-rule, which is configurable with respect to the required length of walls, is applied for this evaluation. In this setting, we tested different configurations of the wall length and different weights for the rules. Table 3 and Table 4 shows the results obtained using different configurations. In the following, the obtained results are discussed in detail.

16

Table 2: Results obtained for the basic structures.

Benchmark	Input map				Meth.	Derived rates				Confusion matrix						Performance	
	o	e	Θ	$\emptyset$		$CorD$	$WroD$	$NotD$	ACC	TP	FP	TN	FN	TPR	TNR	[sec]	[MB]
	17%	76%	1%	5%	BL	84%	11%	6%	89%	26%	2%	63%	9%	74%	96%	0.001	46
					BK	84%	4%	12%	95%	27%	0%	67%	6%	81%	100%	0.018	119
	16%	72%	2%	11%	BL	77%	7%	16%	91%	16%	1%	75%	8%	66%	99%	0.001	47
					BK	87%	5%	9%	95%	18%	0%	77%	5%	78%	100%	0.031	160
	13%	63%	7%	17%	BL	69%	5%	26%	93%	12%	3%	81%	4%	74%	97%	0.001	46
					BK	87%	2%	11%	97%	17%	0%	80%	3%	86%	100%	0.056	224
	15%	80%	1%	5%	BL	78%	14%	9%	85%	23%	3%	60%	14%	63%	95%	0.001	46
					BK	67%	9%	24%	88%	6%	0%	80%	14%	31%	100%	0.017	122
	14%	71%	4%	10%	BL	77%	5%	18%	94%	9%	1%	84%	6%	62%	98%	0.001	46
					BK	78%	4%	17%	95%	4%	0%	90%	6%	38%	100%	0.028	161
	13%	64%	7%	16%	BL	76%	4%	20%	95%	12%	2%	83%	3%	80%	98%	0.001	46
					BK	79%	5%	17%	95%	3%	0%	92%	5%	33%	100%	0.045	218
	23%	71%	0%	5%	BL	81%	12%	8%	87%	30%	3%	58%	10%	76%	96%	0.001	46
					BK	82%	5%	13%	94%	28%	0%	66%	5%	84%	100%	0.019	125
	21%	64%	2%	13%	BL	77%	10%	13%	88%	18%	4%	69%	9%	66%	95%	0.001	45
					BK	79%	10%	11%	89%	19%	2%	69%	11%	65%	98%	0.030	155
	19%	59%	5%	16%	BL	61%	5%	34%	92%	11%	4%	81%	5%	71%	96%	0.001	46
					BK	80%	6%	14%	93%	20%	2%	72%	6%	78%	98%	0.069	229
	17%	78%	0%	4%	BL	79%	8%	12%	90%	26%	1%	66%	7%	79%	98%	0.001	45
					BK	76%	9%	15%	90%	19%	1%	72%	9%	68%	99%	0.022	130
	14%	70%	4%	12%	BL	79%	7%	14%	92%	17%	1%	75%	8%	69%	99%	0.001	47
					BK	77%	11%	12%	88%	9%	0%	78%	12%	44%	100%	0.030	155
	14%	64%	6%	16%	BL	79%	3%	18%	96%	14%	1%	82%	4%	79%	99%	0.001	45
					BK	84%	4%	12%	96%	10%	0%	86%	4%	71%	100%	0.040	186
	26%	68%	1%	5%	BL	79%	9%	13%	90%	41%	4%	50%	4%	91%	92%	0.001	47
					BK	79%	8%	12%	91%	37%	0%	53%	10%	79%	100%	0.020	124
	23%	62%	3%	12%	BL	75%	3%	22%	96%	28%	2%	68%	3%	91%	98%	0.001	47
					BK	86%	5%	9%	95%	26%	0%	68%	5%	83%	100%	0.033	160
	20%	57%	5%	18%	BL	63%	6%	31%	91%	20%	4%	71%	5%	79%	95%	0.002	46
					BK	80%	8%	12%	91%	26%	3%	65%	6%	82%	95%	0.060	222
	33%	61%	1%	6%	BL	79%	7%	14%	92%	60%	3%	32%	5%	93%	91%	0.001	46
					BK	83%	10%	7%	89%	57%	0%	32%	11%	84%	100%	0.021	126
	30%	58%	2%	10%	BL	79%	5%	16%	94%	34%	5%	60%	2%	95%	93%	0.001	46
					BK	91%	4%	6%	96%	37%	0%	59%	4%	91%	100%	0.031	155
	26%	49%	4%	21%	BL	60%	5%	35%	92%	34%	7%	58%	2%	95%	90%	0.001	46
					BK	84%	6%	11%	94%	39%	2%	55%	5%	88%	97%	0.057	197
	14%	81%	1%	4%	BL	83%	6%	11%	94%	28%	0%	65%	7%	81%	100%	0.001	46
					BK	61%	9%	31%	88%	0%	0%	87%	13%	0%	100%	0.017	121
	14%	73%	4%	10%	BL	84%	7%	9%	92%	13%	1%	80%	7%	66%	99%	0.001	45
					BK	75%	8%	17%	90%	0%	0%	90%	10%	0%	100%	0.033	162
	12%	65%	10%	14%	BL	78%	3%	19%	96%	15%	0%	82%	3%	81%	100%	0.002	46
					BK	72%	7%	20%	91%	0%	0%	92%	8%	0%	100%	0.042	198
	28%	64%	1%	7%	BL	88%	5%	7%	94%	36%	2%	59%	3%	92%	96%	0.001	46
					BK	91%	4%	5%	96%	34%	0%	60%	5%	86%	100%	0.020	122
	26%	60%	2%	12%	BL	80%	4%	16%	95%	34%	0%	61%	4%	89%	99%	0.001	46
					BK	88%	5%	7%	95%	35%	0%	59%	5%	87%	99%	0.033	151
	22%	52%	5%	21%	BL	66%	7%	27%	91%	27%	5%	64%	4%	86%	93%	0.001	46
					BK	90%	3%	7%	96%	37%	0%	60%	3%	93%	99%	0.052	193

BL: Baseline filter   BK: Proposed methodology based on background knowledge

Table 3: Results obtained for the office map.

Benchmark	Derived rates				Confusion matrix						Performance	
	CorD	WroD	NotD	ACC	TP	FP	TN	FN	TPR	TNR	[sec]	[MB]
Baseline	38%	21%	41%	64%	29%	6%	34%	30%	49%	85%	0.03	182
C1_a	40%	9%	52%	82%	76%	17%	6%	1%	99%	27%	9	249
C2_a	47%	14%	40%	77%	71%	22%	6%	0%	99%	21%	20	527
C3_a	48%	17%	35%	74%	69%	26%	6%	0%	100%	18%	26	783
C4_a	54%	23%	23%	70%	68%	30%	2%	0%	100%	7%	16	255
C5_a	65%	32%	4%	67%	66%	33%	1%	0%	100%	3%	18	264
C1_b	33%	7%	60%	83%	66%	8%	17%	9%	88%	66%	13	252
C2_b	45%	13%	42%	77%	67%	18%	10%	5%	93%	36%	26	532
C3_b	42%	15%	43%	73%	63%	22%	10%	5%	93%	30%	42	781
C4_b	55%	22%	22%	71%	65%	27%	6%	2%	96%	19%	24	251
C5_b	67%	30%	3%	70%	65%	30%	4%	1%	99%	13%	39	262

The office map contains 5% occupied cells, 90% empty cells, 1% unknown cells, and 4% conflicting cells.

Office-map. The *office-map* was generated by Evidential FastSLAM based on simulation data. This has the advantage that the ground truth map is known. The robot in the simulation environment[7] has similar properties as a real one in terms of sensor noise and its dynamics. The resulting map consists of 188×259 grid cells with a resolution of $5\,cm$ per cell, where 1% of them remain unknown and 4% of them remain in conflict after applying Eq. (8). Figure 5 shows the input-map m^Y, the derived-map m^D for configuration C5_a, the derived-map using the base line filter, and the ground truth-map m^{GT}. As above, occupied cells are shown in black, empty cells are shown in white, conflicting cells are shown in red, and unknown cells are shown in gray. These figures clearly show that the proposed methodology is capable to correctly reduce the uncertainty. The "wall"-rule reduces uncertain cells along walls by correctly detecting them and by assigning the mass of these cells occupied. Accordingly, the "empty grid"-rule correctly detects uncertain grid cells surrounded by areas with mass assigned empty and in turn assigns the mass of these grid cells to empty.

All results for the *office-map* are summarized in Table 3, which presents results for differently weighted rules. In the configurations with suffix "_a", we assigned the generalized "wall"-rule a higher weight than the "empty subgrid"-rule. On the other hand, in the configurations with suffix "_b", we assigned the "empty subgrid"-rule a higher weight than the "wall"-rule. In addition, we configured the generalized "wall"-rule differently and list the results in rows C1 to C5. More precisely, we tested five different configurations in which we varied the number of occupied cells needed in order to categorize a row or column as wall to be between 2% and 12% of the grid width.

We can observe that the weights have an impact. Especially, the percentage of false-negative cells (column *FN*) is impacted by the different weights, i.e. FN is much lower for the configurations with suffix "_a". This is an important criterion for path planning of an actual robot, because every false-negative cell is falsely classified to be empty. As a result, the planned path would be suboptimal, since once the robot detects that the cell is occupied, it has to re-plan and make a detour to avoid a collision. Hence, the evaluations show that the configurations with suffix "_a" are especially suited for path planning as *FN* is always less than 1%. With respect to the different configurations of the "wall"-rule, we observe that the shorter the wall length, the lower the percentage of *not* derived cells (column *NotD*), because more walls are detected by the rule. For this

---

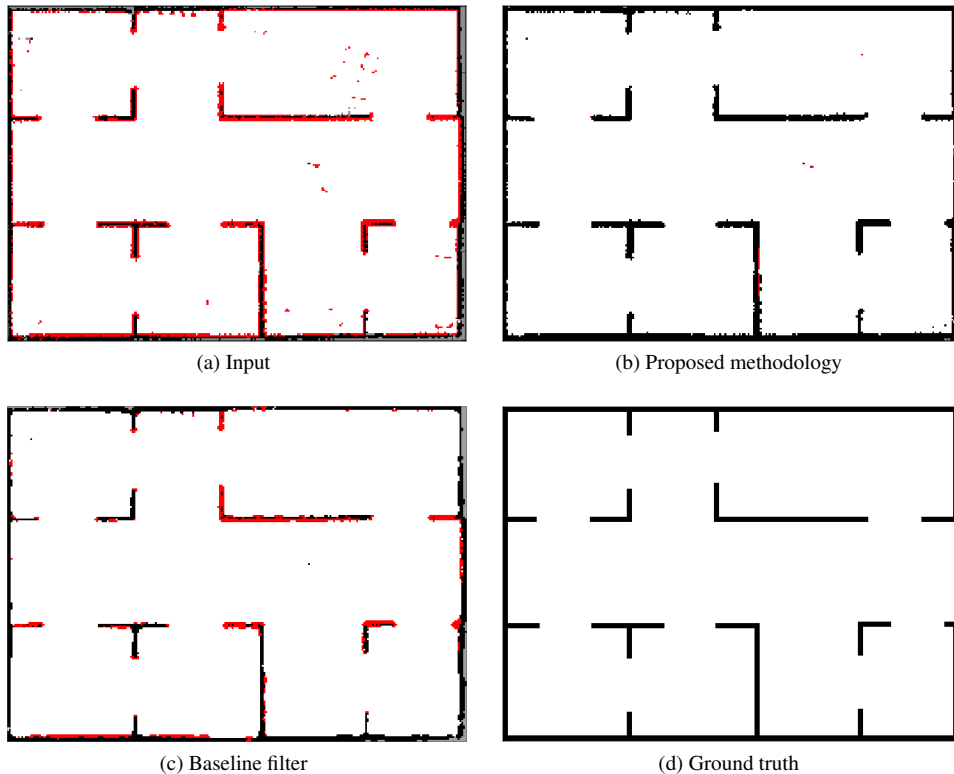[7]We used GridmapNavSim from the Mobile Robot Programming Toolkit (see http://www.mrpt.org).

Figure 5: Input map, map derived with the proposed methodology, map derived with the baseline filter, and ground truth map for the *Office-map*.

office-map, a shorter wall length gives high numbers of correctly derived cells (column *CorD*), but also increases the misclassified cells (column *WroD*).

Overall, the numerical summary in Table 3 confirms that the proposed methodology achieves a high accuracy (between 67% and 83% depending on the configuration) and that a huge amount of uncertain cells is correctly derived (between 33% and 67% in column *CorD*). Furthermore, the results show that the proposed methodology outperforms the baseline filter in almost all configurations and quality criteria. It is capable of correctly deriving up to 67% of the uncertain cells, while the baseline filter correctly derives 38%. This confirms the effectiveness of the applied rules and the proposed methodology.

Intel-map. The *intel-map* was generated by the Evidental FastSLAM algorithm based on the popular community dataset of the Intel Research Lab provided by Dirk Hähnel[8]. It was recorded in 44:51 minutes (according to the log file) using a Pioneer 2 robot equipped with a SICK LMS laser range finder. The resulting map is even larger than the *office-map* and has a size of 569×567 grid cells with a resolution of 5 cm per cell. This map serves as input for the proposed methodol-

---

[8]Available online at `http://www2.informatik.uni-freiburg.de/~stachnis/datasets.html`

Table 4: Results obtained for the Intel-map.

Benchmark	Derived rates				Confusion matrix						Performance	
	CorD	*WroD*	*NotD*	*ACC*	*TP*	*FP*	*TN*	*FN*	*TPR*	*TNR*	[sec]	[MB]
Baseline	15%	3%	82%	84%	13%	12%	70%	4%	76%	85%	0.1	627
C1	33%	4%	63%	89%	4%	2%	85%	9%	33%	97%	4616	2230
C2	34%	5%	61%	88%	7%	4%	81%	8%	46%	95%	5479	2217
C3	36%	5%	59%	88%	12%	5%	76%	7%	61%	94%	7340	2292
C4	39%	8%	53%	84%	17%	10%	67%	6%	72%	87%	10623	2253
C5	37%	7%	56%	85%	13%	8%	72%	7%	65%	90%	7542	2221

The Intel-map contains 5% occupied cells, 57% empty cells, 28% unknown cells, and 10% conflicting cells.

Figure 6: The input map for the *Intel-map*.

ogy (shown in Figure 6) and contains 28% unknown and 10% conflicting cells. Since no ground truth map is available for this dataset, an estimation has manually been created.

Table 4 summarizes the results for five selected configurations. In these configurations, we also vary the settings of the generalized "wall"-rule. For example, C1 uses 4% of the grid width in order to detected a wall, where C5 uses much shorter walls (only 1% of the grid width). We again observer that, in general, shorter wall lengths cause less not-derived cells (column *NotD*) but increase the percentage of misclassified cells (column *WroD*).

When considering all five configurations, the methodology is able to correctly derive cells (between 33% and 39% depending on the configuration), although this map contains a high percentage of uncertainty. It is noteworthy that the rules almost do not derive any wrong assignments (i.e. *WroD* is less than 8% in all configurations), which results in high accuracies (between 84% and 89% depending on the configuration). Comparing the results to the baseline, the proposed methodology is capable of correctly deriving more than twice as much cells than the baseline filter in all configurations.

Moreover, all these results have been determined in acceptable run-times (i.e. between a few seconds and up to a few hours) and with a limited amount of memory consumption (between few megabytes and up to approx. two gigabytes). Both, the run-times and the memory consumptions depend on the size of the input map and the number of applied rules.

Overall, the results show the efficiency of the proposed methodology, which is especially powerful for real-world maps. Each of the selected configurations produces different results and, which of the configuration is the "best", depends on the underlying application and requirements.

7. Conclusion

In this work, we considered reasoning and uncertainty reduction. It has been discussed that the full potential of the available information is usually not exploited by existing approaches, since utilizing all background and expert knowledge eventually results in a computationally complex task. In order to overcome these limitations, we proposed the exploitation of formal methods. More precisely, we formalized background and expert knowledge about a particular environment by the means of rules, which are used to reduce the uncertainty in evidential grid maps after the fusion process and reason about the true state of the cells. Therefore, three rules for the use in the context of office environments have been presented.

The proposed methodology was evaluated and compared with a baseline using different scenarios: We first considered hand-crafted benchmarks representing basic structures that can be found in office environments. Then, we demonstrated the applicability to practically relevant tasks by the use of two real-world maps. In all evaluations, our methodology was able to significantly reduce the uncertainty of the input maps. Moreover, we showed not only that it can be applied to small examples, but also that it performs best on maps of a practically relevant size and with a realistic uncertainty distribution.

Next steps are the formalization of further rules as already discussed in the paper. Furthermore, the application to other domains may require a completely new set of rules, which has to be provided by domain experts. For example, in the context of autonomous driving [21, 23], the knowledge about typical structures, like roads, rows of houses, or other cars can be encoded. Another interesting application is the reduction of uncertainty in maps derived from aerial or satellite images [39, 40, 41], which requires contextual information about man-made structures, agricultures, forests, rivers, seas, or mountains.

Another promising future work is to extend the proposed methodology for the use with non-categorical mass functions. This can either be implemented by a discretization of the mass values or by extending the current methodology to choose the weights of the rules dependent on the real mass. Both ideas are promising directions, but require an adaption of the rules. Furthermore, in this work, we put the focus on unknown and conflicting cells in order to reduce the uncertainty in the map. But, our methodology can also be extended to consider the expert knowledge as a general information source and, accordingly, correct occupied and empty cells as well. Finally, the proposed methodology is not limited to uncertainty reduction in the context of map-like data, but can also be applied to more general tasks that involve uncertain information.

References

[1] B. Khaleghi, A. Khamis, F. O. Karray, S. N. Razavi, Multisensor data fusion: A review of the state-of-the-art, Journal on Information Fusion 14 (1) (2013) 28–44.

[2] S. Thrun, W. Burgard, D. Fox, Probabilistic robotics, MIT Press, Cambridge, MA, 2005.

[3] S. Thrun, Robotic mapping: A survey, Exploring artificial intelligence in the new millennium 1 (2002) 1–35.

[4] J. Clemens, R. Wille, K. Schill, Towards the exploitation of formal methods for information fusion, in: SPIE: Multisensor, Multisource Information Fusion: Architectures, Algorithms, and Applications, Vol. 9872, 2016, pp. 987202–1–987202–10.

[5] D. S. Johnson, Approximation algorithms for combinatorial problems, Journal of Computer and System Sciences 9 (3) (1974) 256–278.

[6] P. Hansen, B. Jaumard, Algorithms for the maximum satisfiability problem, Journal of Computing 44 (4) (1990) 279–303.

[7] A. Elfes, Using occupancy grids for mobile robot perception and navigation, Journal of Computer 22 (6) (1989) 46–57.

[8] D. Pagac, E. M. Nebot, H. Durrant-Whyte, An evidential approach to map-building for autonomous vehicles, IEEE Trans. on Robotics and Automation 14 (4) (1998) 623–629.

[9] G. Shafer, A mathematical theory of evidence, Princeton University Press, 1976.

[10] W. Yaonan, Y. Yimin, Y. Xiaofang, Z. Yi, Z. Yuanli, Y. Feng, T. Lei, Autonomous mobile robot navigation system designed in dynamic environment based on transferable belief model, Measurement 44 (8) (2011) 1389–1405.

[11] J. Clemens, T. Reineking, T. Kluth, An evidential approach to SLAM, path planning, and active exploration, Journal of Approximate Reasoning 73 (2016) 1–26.

[12] T. Reineking, J. Clemens, Dimensions of uncertainty in evidential grid maps, in: Spatial Cognition IX, Vol. 8684 of Lecture Notes in Computer Science, Springer, 2014, pp. 283–298.

[13] P. Smets, R. Kennes, The transferable belief model, Journal of Artificial Intelligence 66 (1994) 191–234.

[14] M. Ribo, A. Pinz, A comparison of three uncertainty calculi for building sonar-based occupancy grids, Journal on Robotics and Autonomous Systems 35 (3-4) (2001) 201–209.

[15] X. Li, X. Huang, J. Dezert, L. Duan, M. Wang, A successful application of DSmT in sonar grid map building and comparison with DST-based approach, Journal of Innovative Computing, Information and Control 3 (3) (2007) 539–549.

[16] T. Yang, V. Aitken, Evidential mapping for mobile robots with range sensors, IEEE Trans. on Instrumentation and Measurement 55 (4) (2006) 1422–1429.

[17] J. Moras, J. Dezert, B. Pannetier, Grid occupancy estimation for environment perception based on belief functions and PCR6, in: SPIE: Signal Processing, Sensor/Information Fusion, and Target Recognition, Vol. 9474, 2015, pp. 94740P–94740P.

[18] J. Mullane, M. D. Adams, W. S. Wijesoma, Evidential versus bayesian estimation for radar map building, in: Int'l Conf. on Control, Automation, Robotics and Vision, 2006, pp. 1–8.

[19] T. Ike, B. Grabe, F. Knigge, M. Hoetter, Evidence-based analysis of internal conflicts from inverse sensor models, in: IEEE Intelligent Vehicles Symposium, 2009, pp. 1236–1240.

[20] J. Moras, V. Cherfaoui, P. Bonnifait, Credibilist occupancy grids for vehicle perception in dynamic environments, in: Int'l Conf. on Robotics and Automation, 2011, pp. 84–89.

[21] M. Kurdej, J. Moras, V. Cherfaoui, P. Bonnifait, Controlling remanence in evidential grids using geodata for dynamic scene perception, Journal of Approximate Reasoning 55 (1, Part 3) (2014) 355 – 375.

[22] M. Kurdej, J. Moras, V. Cherfaoui, P. Bonnifait, Map-aided evidential grids for driving scene understanding, IEEE Intelligent Transportation Systems Magazine 7 (1) (2015) 30–41.

[23] R. Jungnickel, M. Köhler, F. Korf, Efficient automotive grid maps using a sensor ray based refinement process, in: IEEE Intelligent Vehicles Symposium, 2016, pp. 668–675.

[24] H. Durrant-Whyte, T. Bailey, Simultaneous localization and mapping: Part I, IEEE Robotics & Automation Magazine 13 (2) (2006) 99–110.

[25] T. Reineking, J. Clemens, Evidential FastSLAM for grid mapping, in: Int'l Conf. on Information Fusion, 2013, pp. 789–796.

[26] M. Montemerlo, S. Thrun, D. Koller, B. Wegbreit, FastSLAM: A factored solution to the simultaneous localization and mapping problem, in: Proc. of the National conference on Artificial Intelligence, 2002, pp. 593–598.

[27] D. Hähnel, W. Burgard, D. Fox, S. Thrun, An efficient FastSLAM algorithm for generating maps of large-scale cyclic environments from raw laser range measurements, in: Int'l Conf. on Intelligent Robots and Systems, Vol. 1, IEEE, 2003, pp. 206–211.

[28] R. R. Yager, On the Dempster-Shafer framework and new combination rules, Journal on Information Sciences 41 (2) (1987) 93–137.

[29] A. Martin, C. Osswald, A new generalization of the proportional conflict redistribution rule stable in terms of decision, in: Advances and Applications of DSmT for Information Fusion, Vol. 2, 2006, pp. 69–88.

[30] T. Denœux, Conjunctive and disjunctive combination of belief functions induced by nondistinct bodies of evidence, Journal of Artificial Intelligence 172 (2-3) (2008) 234–264.

[31] G. Grisetti, C. Stachniss, W. Burgard, Improved techniques for grid mapping with Rao-Blackwellized particle filters, IEEE Trans. on Robotics 23 (1) (2007) 34–46.

[32] J. Marques-Silva, T. Glass, Combinational equivalence checking using Boolean satisfiability and recursive learning, in: Design, Automation and Test in Europe, 1999, pp. 145–149.

[33] P. Williams, A. Biere, E. Clarke, A. Gupta, Combining decision diagrams and SAT procedures for efficient symbolic model checking, in: Computer Aided Verification, Vol. 1855 of LNCS, Springer Verlag, 2000, pp. 124–138.

[34] S. Eggersglüß, R. Wille, R. Drechsler, Improved SAT-based ATPG: more constraints, better compaction, in: Int'l Conf. on CAD, 2013.

[35] G. Tseitin, On the complexity of derivation in propositional calculus, in: Studies in Constructive Mathematics and Mathematical Logic, Part 2, 1968, pp. 115–125, (Reprinted in: J. Siekmann, G. Wrightson (Ed.), Automation of Reasoning, Vol. 2, Springer, Berlin, pp. 466-483, 1983.).

[36] N. Eén, N. Sörensson, Translating pseudo-Boolean constraints into SAT, Journal on Satisfiability, Boolean Modeling and Computation 2 (1-4) (2006) 1–26.

[37] L. M. de Moura, N. Bjørner, Z3: An Efficient SMT Solver, in: Tools and Algorithms for Construction and Analysis of Systems, 2008, pp. 337–340.

[38] Z. Fu, S. Malik, On solving the partial MAX-SAT problem, in: Int'l Conf. on Theory and Applications of Satisfiability Testing, 2006, pp. 252–265.

[39] A. Sarkar, A. Banerjee, N. Banerjee, S. Brahma, B. Kartikeyan, M. Chakraborty, K. L. Majumder, Landcover classification in MRF context using Dempster-Shafer fusion for multisensor imagery, IEEE Trans. on Image Processing 14 (5) (2005) 634–645.

[40] F. Rottensteiner, J. Trinder, S. Clode, K. Kubik, Using the Dempster-Shafer method for the fusion of LIDAR data and multi-spectral images for building detection, Journal on Information Fusion 6 (4) (2005) 283–300.

[41] G. Sohn, I. Dowman, Data fusion of high-resolution satellite imagery and LiDAR data for automatic building extraction, ISPRS Journal of Photogrammetry and Remote Sensing 62 (1) (2007) 43–63.